

**Quantized electronic structure and growth of Pb films on highly oriented pyrolytic graphite**Y. Liu,<sup>1,2</sup> J. J. Paggel,<sup>3</sup> M. H. Upton,<sup>4</sup> T. Miller,<sup>1,2</sup> and T.-C. Chiang<sup>1,2</sup><sup>1</sup>*Department of Physics, University of Illinois at Urbana-Champaign, 1110 West Green Street, Urbana, Illinois 61801-3080, USA*<sup>2</sup>*Frederick Seitz Materials Research Laboratory, University of Illinois at Urbana-Champaign, 104 South Goodwin Avenue, Urbana, Illinois 61801-2902, USA*<sup>3</sup>*Continental Automotive GmbH, Regensburg 93055, Germany*<sup>4</sup>*Advanced Photon Source, Argonne National Laboratory, 9700 South Cass Avenue, Argonne, Illinois 60439, USA*

(Received 15 August 2008; revised manuscript received 20 October 2008; published 31 December 2008)

We have measured the electronic structure of thin Pb films grown on highly oriented pyrolytic graphite (HOPG) by angle-resolved photoemission spectroscopy. Quantum well states (QWSs) corresponding to confined Pb valence electrons are observed. Their energy positions are fixed, but their intensities evolve for increasing Pb coverages. The results indicate that the films are rough, consisting of multiple thicknesses. Nevertheless, the thickness distribution is sufficiently narrow to allow a unique assignment for each QWS peak in terms of a quantum number and the exact film thickness in atomic layers. For increasing Pb coverages of up to 10 monolayers (ML), the even film thicknesses of 2, 4, 6, 8, and 10 ML are much more prevalent than the odd film thicknesses of 1, 3, 5, 7, and 9 ML, thus suggesting significant differences in surface energy between the even and odd thicknesses. These results are consistent with an available first-principles calculation of the surface energies of freestanding films; an implication is that the interaction between the Pb film and the HOPG substrate is weak. The in-plane dispersion relations of the QWSs are measured. The effective masses at the surface zone center agree well with the results calculated from the bulk Pb band structure, in sharp contrast to the strongly enhanced or anomalous effective masses in Pb films grown on Si(111) as reported previously. This finding indicates that the anomalous effective masses in Pb/Si(111) are not caused by increased electron correlation effects in a confined geometry, but are rather attributable to a strong interfacial interaction between the QWSs and the substrate electronic structure.

DOI: [10.1103/PhysRevB.78.235437](https://doi.org/10.1103/PhysRevB.78.235437)

PACS number(s): 73.21.Fg, 73.20.At, 79.60.Dp

**I. INTRODUCTION**

Ultrathin metal films grown on semiconductor and metal substrates have attracted considerable interest because of their often novel physical behavior and properties. Electrons in such films form standing waves, or quantum well states (QWSs), for energies within substrate band gaps.<sup>1-4</sup> The discreteness of the electronic structure can result in large variations in the density of states near the Fermi level as a function of film thickness, in turn affecting the charge distribution, electronic energy, and physical properties.<sup>5</sup> Electronic states outside the substrate band gaps are not confined, but they can form quantum well resonances provided that there is a substantial mismatch in electronic band structure between the film and the substrate. These resonance states are essentially broadened QWSs, and they too can contribute to the layer-by-layer variations in physical properties. For both QWSs and resonances, the substrate is an integral part of the quantum system. It provides a confinement potential or potential step as seen by the valence electrons in the film; additionally it can affect the detailed electronic structure of the system through a variety of effects including interface scattering,<sup>6</sup> umklapp reflection,<sup>7-9</sup> and hybridization and coherent electronic coupling across the interface.<sup>10-13</sup>

The present work is a study using angle-resolved photoemission of the quantum confinement effects in Pb(111) films deposited on highly oriented pyrolytic graphite (HOPG). There is considerable prior photoemission work on Pb films deposited on the Si(111)-(7×7) surface.<sup>14-17</sup> The main difference between Pb/HOPG and Pb/Si is that the

former has a relatively weak interfacial interaction based on two observations. First, graphite is a layered material with weak bonding in-between graphene layers. When it is cleaved to expose a surface, the electrons near the surface do not undergo much adjustment, and the top graphene layer is stable. By contrast, the Si(111) surface is heavily reconstructed to minimize the dangling-bond energies. The remaining dangling bonds are active and can bind strongly to an overlayer. Second, the Si band gap below the Fermi level available for quantum confinement is typically less than 1 eV. Overlayer states below the gap can readily couple to the Si electronic states. By contrast, graphite has a large band gap at the surface zone center extending over the entire width of the Pb *p* valence band below the Fermi level. The *p* valence electrons of Pb are thus largely decoupled from the substrate, but not entirely. Because the Pb and graphite lattices are incommensurate, mixing of the in-plane wave vectors can lead to an effective coupling when the three-dimensional band structure of graphite is considered. Strictly speaking, the QWSs seen in Pb/graphite are resonance states, but this is a minor effect.

One reason for our interest in Pb/graphite is its weak interfacial coupling that makes an interesting comparison to Pb/Si. Our results show that the energies of the QWSs are substantially different for the two cases. The growth mode is also very different, even though an electronic growth behavior is apparent in both cases. Furthermore, the effective masses of the QWS subbands at the surface zone center are substantially different. The Pb/Si system is known for its anomalously large (or even negative) effective masses, and the physics is still under debate.<sup>14,15</sup> In the present work, we

show that the effective masses in Pb/graphite are quite normal. Thus, the anomalous results in Pb/Si cannot be attributed to enhanced electron correlation effects in a confined geometry. Rather, the strong interaction between the Pb film and the Si substrate is the cause.

Another motivation for our work is the prevailing interest in graphene-based materials.<sup>18</sup> Graphene sheets and stacks have unusual properties possibly suitable for advanced electronic applications. Metallization and film formation on graphene/graphite is essential for integrating such materials into useful device configurations. There is an earlier study of Pb films deposited on a graphene-terminated SiC(0001) surface.<sup>19</sup> It is interesting to make a comparison and determine what differences might arise between the two substrates. For the most part, the QWS structure is similar, but there are differences in growth behavior. It should be noted that graphene/graphite has been employed as a substrate material in previous studies of quantum well states in Ag and alkali-metal films.<sup>20–23</sup>

## II. EXPERIMENTAL DETAILS

The photoemission measurements were performed at the Synchrotron Radiation Center, University of Wisconsin–Madison. HOPG pieces of grade ZYA were purchased from Advanced Ceramics. The material is composed of graphite crystallites highly oriented, within  $0.4^\circ$ , along the  $c$  axis, but the in-plane orientation of the crystallites is completely random. The typical crystallite size is 1 to 10  $\mu\text{m}$  in the basal plane and  $>0.1 \mu\text{m}$  perpendicular to the basal plane.<sup>24</sup> A small piece of the HOPG sample was mounted on a Si(111) substrate, which served as a Joule heater for the sample. The HOPG sample was cleaved *ex situ* using a piece of sticky tape, and then transferred immediately into the vacuum chamber. It was degassed at about  $550^\circ\text{C}$  for several hours and the observed reflection high-energy electron diffraction (RHEED) pattern showed very sharp diffraction rings, characteristic of a clean HOPG surface. A thermal evaporation source was used to deposit Pb onto the sample surface at  $\sim 115 \text{ K}$  at a rate of  $0.46 \text{ \AA}/\text{min}$  as determined from a quartz-crystal thickness monitor. The evaporation source consisted of ultrapure Pb contained in a tungsten crucible, which was heated by a feedback-controlled electron beam. The thickness monitor, while quite precise, was calibrated to only within about 20% accuracy.

The photoemission data were acquired with the sample at  $\sim 115 \text{ K}$  using a Scienta SES 100 analyzer equipped with a two-dimensional detector that yielded photoemission intensities as a function of electron energy and emission angle along a selected azimuthal direction.<sup>25</sup> The sample normal was tilted relative to the analyzer axis in steps of  $4^\circ$  to create overlapping data sets, which were later stitched together to yield an intensity map over a wide range of emission angle. For a determination of the effective masses of the bands, a transformation of the data was made to convert the emission angle into in-plane wave vector. All data shown below were taken with a photon energy of 22 eV.

## III. RESULTS AND DISCUSSION

Cuts of the intensity maps at normal emission for nominal Pb film coverages ranging from 0.5 to 10 monolayers (ML);

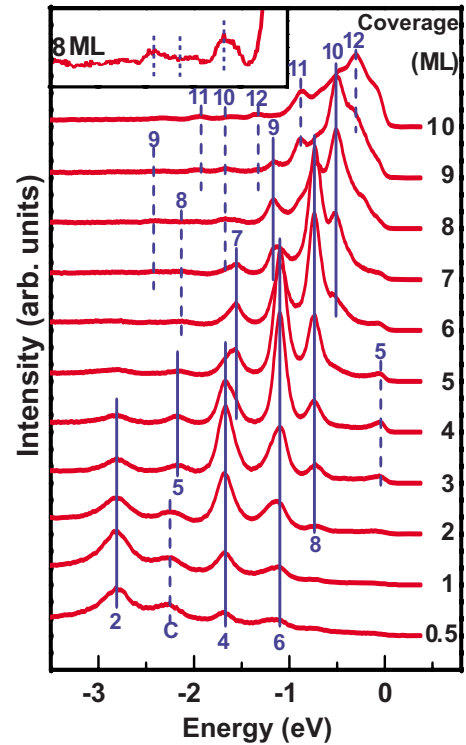


FIG. 1. (Color online) Normal emission spectra for Pb films grown on HOPG at various nominal Pb coverages. The photon energy used was 22 eV. The QWS peaks are marked by the corresponding film thicknesses. Peaks that are marked by the solid lines are analyzed to yield the results shown in Fig. 3. The peak marked by “C” is derived from the HOPG substrate. The inset is an enlarged view of the 8-ML spectrum to show the weaker peaks.

in terms of the bulk Pb lattice) are displayed in Fig. 1. Already at 0.5-ML coverage, multiple Pb-derived QWS peaks emerge. Note that the peak marked by “C” is derived from the HOPG substrate, and its origin is unclear.<sup>26</sup> As the Pb coverage increases, the QWS peak intensities vary but the peak positions remain unchanged. Generally, each peak can be observed over a range of several MLs of Pb coverage; thus, the film thickness corresponding to the particular peak (marked in Fig. 1) is present over the same coverage range. An immediate conclusion is that the film growth mode is three dimensional involving simultaneously several thicknesses centered about the nominal film coverage. For comparison, Pb films grown on Si(111) can be atomically uniform under the right conditions.<sup>16</sup>

This three-dimensional growth mode does not allow a simple assignment of the QWS peaks to different thicknesses. Nevertheless, a unique assignment can be reached based on several constraints. The energies of the QWSs are determined by the Bohr-Sommerfeld quantization rule,<sup>2</sup>

$$2k_{\perp}(E)Nt + \varphi_i(E) + \varphi_s(E) = 2n\pi \quad (1)$$

where  $k_{\perp}(E)$  is the perpendicular component of the wave vector of the electron at energy  $E$ ,  $N$  is the film thickness in monolayers,  $t$  is the monolayer thickness,  $n$  is a quantum number, and  $\varphi_i$  and  $\varphi_s$  are the phase shifts at the interface and surface, respectively.  $k_{\perp}(E)$  is determined by the bulk

band structure of Pb along the [111] direction.  $\varphi_s(E)$  is available from a first-principles calculation.<sup>27</sup>  $\varphi_i(E)$  is not known, but it should be a smooth function and not too different from  $\varphi_s(E)$  because of the weak interaction between the film and the substrate; we employ a second-order polynomial as a fitting function. With a reasonable guess of  $\varphi_i(E)$ , QWS peak positions from Eq. (1) are in fairly good agreement with the observed peak positions for the range of  $N$  expected based on the nominal Pb coverage. The peak assignments in terms of  $N$  and  $n$  are then made, and the polynomial coefficients in  $\varphi_i(E)$  are varied for a best fit to the observed peak positions.

The experimentally observed QWS peak positions and the results from the fit are shown in Fig. 2(a); the agreement is excellent. No peaks are observed for  $N=1$  and 3, which will be addressed in connection with the growth behavior below.  $\varphi_i(E)$  determined from the fit and  $\varphi_s(E)$  from a first-principles calculation are both shown in Fig. 2(b). Indeed, the two functions are not very different. In a sense, the Pb-graphite interface is not too different from a Pb-vacuum interface. Figure 2(c) compares the QWS peak energies with those for Pb films grown on graphene-terminated SiC(0001) and Si(111).<sup>16,19</sup> The results for Pb/HOPG and Pb/SiC are very close. The main difference is that the QWS peaks for  $N=5, 7,$  and  $9$  are clearly seen in Pb/HOPG, but not in Pb/SiC. The results for Pb/Si are quite different. Only peaks within about 1 eV below the Fermi level are observed. This observation can be related to the relatively small gap in Si available for quantum confinement. Resonances at lower energies are too broad to be detected. The significant differences in the observed QWS energies can be attributed to a different phase-shift function  $\varphi_i(E)$  in Pb/Si; this phase shift is expected to change rapidly near the Si band edge.

The growth behavior can be deduced from the QWS peak intensities, each of which should be proportional to the surface area of the corresponding film thickness. The spectra in Fig. 1 are fitted with Voigt line shapes, and the resulting intensities of the most prominent peaks, marked by the solid vertical lines, are plotted in Fig. 3(a) as a function of the nominal film coverage. In general, each peak for thickness  $N$  reaches its maximum intensity at a Pb coverage around  $N$ , as expected. The peaks corresponding to even- $N$  thicknesses are much more intense than the odd- $N$  thicknesses. Since some of the peak intensities (odd ML cases) are too small to be displayed clearly in this plot, the data are replotted in Fig. 3(b). Here, the intensity of each peak is self-normalized to its maximum peak intensity within the range, and the results for different  $N$  are offset vertically to show the relative peak intensity evolution. In each case, the peak intensity goes through a maximum with a width of 2–4 ML, which is approximately an indication of the width of the film thickness distribution.

The weak odd- $N$  peak intensities indicate that the system favors the formation of even- $N$  thicknesses. This can be understood in terms of Fig. 4(a), which displays the surface energies for different thicknesses of freestanding Pb films based on a first-principles calculation.<sup>27</sup> While Pb films on HOPG are not freestanding, the results should be similar. The damped bilayer oscillations in surface energy as shown in the calculation are well-known effects—the one-dimensional equivalent of the “shell effect.”<sup>5</sup> It is related to

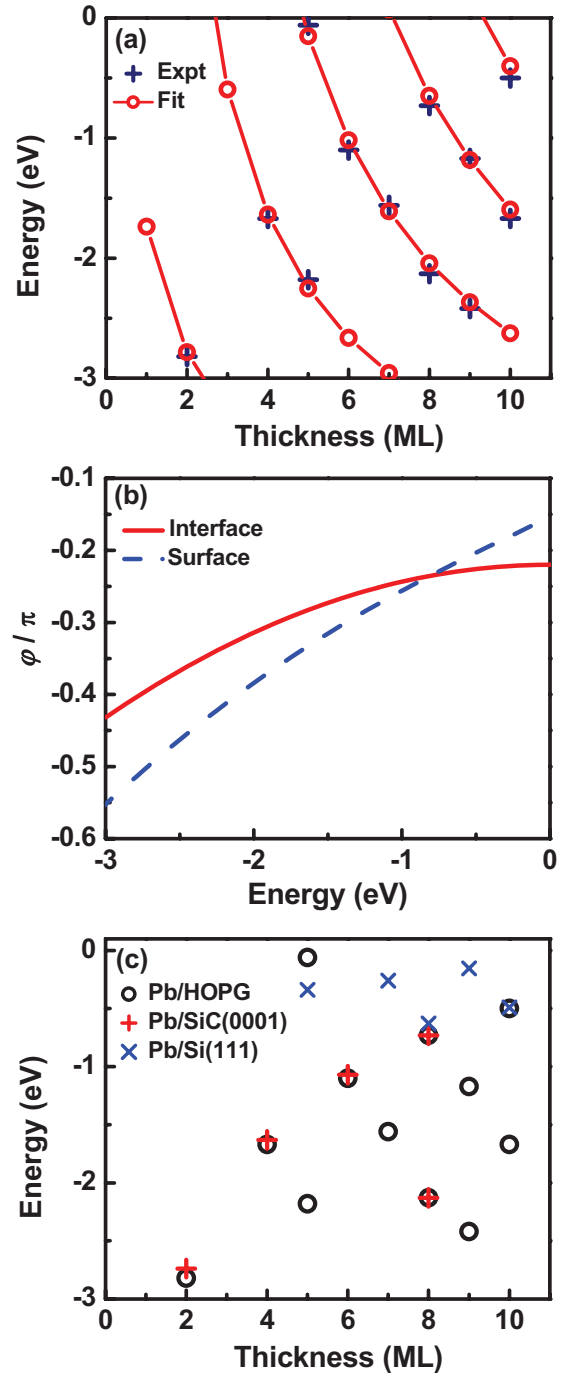


FIG. 2. (Color online) (a) Experimental and fitted energies of QWSs as a function of film thickness. (b) Phase shifts at the surface and interface, in units of  $\pi$ . (c) Comparison of QWS energies for Pb films on HOPG, SiC, and Si.

the quantum well electronic structure of the Pb films, and the bilayer period is just one half of the Fermi wavelength of Pb along the [111] direction. The calculated surface energies for odd  $N$  are generally higher than those for nearby even  $N$ , which accounts for the preference of even  $N$  thicknesses. Furthermore, the surface energies for  $N=1$  and  $3$  are much higher than the rest, thus accounting for the absence of QWS peaks corresponding to  $N=1$  and  $3$  in the data. At higher thicknesses, the even-odd selection becomes less pronounced

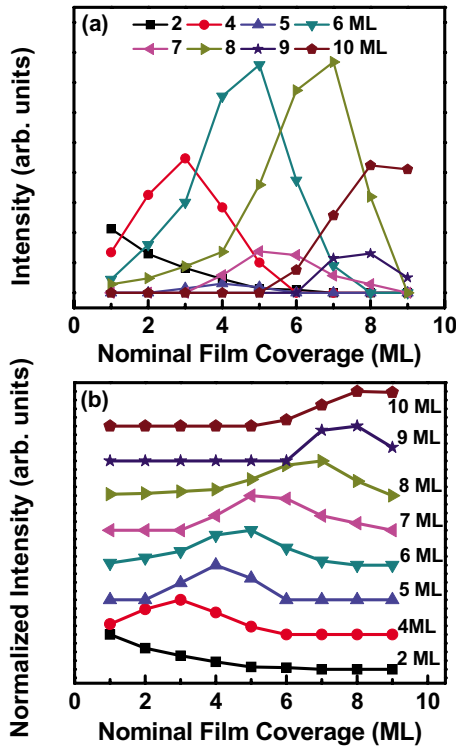


FIG. 3. (Color online) (a) Intensity evolution of the QWS peaks marked by the solid vertical lines in Fig. 1 for different film thicknesses as a function of the nominal Pb film coverage. (b) Self-normalized QWS peak intensities as a function of the nominal Pb film coverage.

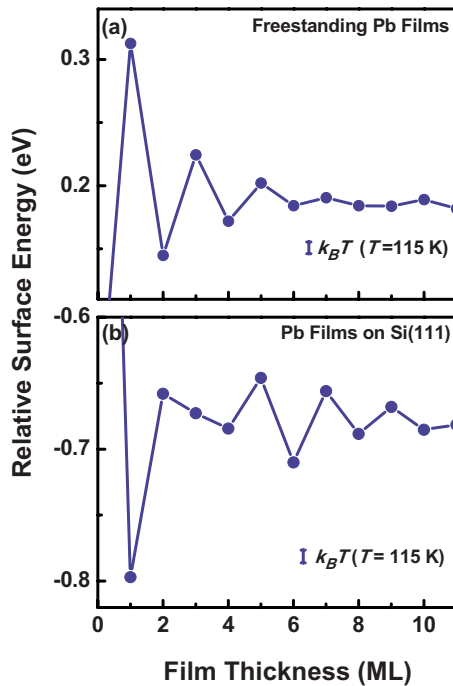


FIG. 4. (Color online) Relative surface energies as a function of film thickness, based on a first-principles calculation for (a) freestanding Pb films and (b) Pb films on Si(111).

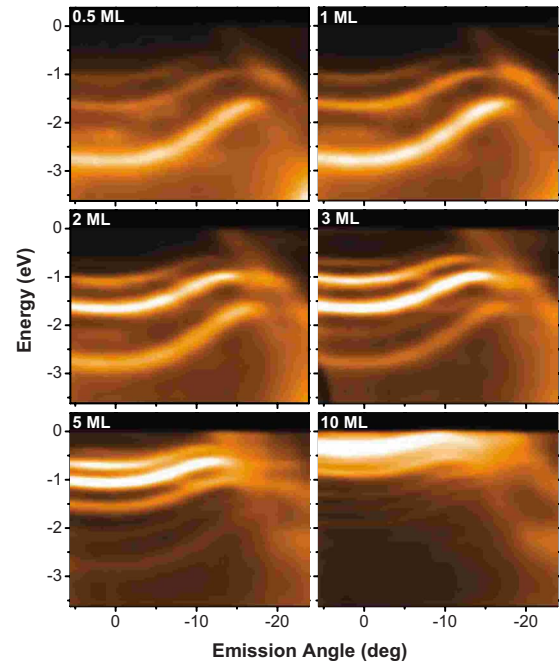


FIG. 5. (Color online) Photoemission intensity maps as a function of energy and emission angle for nominal Pb film coverages of 0.5, 1, 2, 3, 5, and 10 ML.

because of the damping of the quantum oscillations in surface energy. Note that film growth is not just affected by the energetics; kinetics can also play a role.<sup>28</sup> In the present case, energetics alone explains the major features of the growth behavior.

The trend of growth for Pb/HOPG is very similar to that found for Pb/SiC. The main difference is that the  $N=5$ , 7, and 9 peaks are completely missing in the latter case. It is also interesting to note that for Pb growth on Si(111) at similar temperatures,  $N=1$  and 6 (or  $N=1$  and 8, depending on the exact growth conditions) are very much preferred.<sup>16,29–31</sup> The reason is that the Pb-Si interface corresponds to a very different boundary condition. The bilayer oscillations in surface energy have a different phase shift. As a result, the lowest surface energies occur at  $N=1$  and 6, as shown in Fig. 4(b) based on a first-principles calculation.<sup>29</sup>

The in-plane dispersion relations for the QWSs are shown in Fig. 5 for a number of nominal film coverages; each case corresponds to a few different  $N$ . The spectral peaks as a function of energy are quite sharp near  $\bar{\Gamma}$ , but they become blurred at large emission angles. Since the crystallites in HOPG are randomly oriented within the surface plane, the Pb domains are also randomly oriented. The in-plane dispersion relations of the QWSs generally depend on the azimuthal direction relative to the Pb lattice. The random alignment is at least partly the reason for the blurring of the spectra at large emission angles.

For reference, Fig. 6 shows the projected bulk band structure of a 9-ML Pb(111) slab, which should be a good approximation for the general shapes of the QWS dispersion relations (aside from a phase shift). The lowest fully occupied band is an  $s$  band. The  $p$  band starts at about  $-4$  eV and spans the Fermi level. The QWSs derived from the  $p$  band

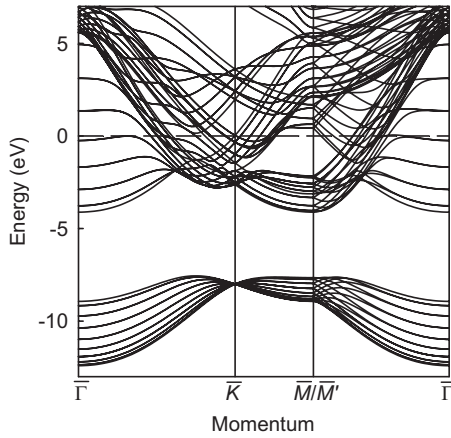


FIG. 6. Projected bulk band structure of a 9-ML Pb film.

have nearly the same dispersion relations along the two major symmetry directions  $\bar{\Gamma}\bar{M}$  and  $\bar{\Gamma}\bar{K}$  near the zone center  $\bar{\Gamma}$ , but the results differ at large emission angles. The overall shapes of the QWS dispersion relations look very similar to the projected band structure.

Since the symmetry of Pb(111) at  $\bar{\Gamma}$  is high (threefold), the effective masses of the QWS subbands are isotropic within the surface plane. An analysis of the curvatures at  $\bar{\Gamma}$  of the most prominent bands in the data yields the corresponding effective masses. The results, normalized to the free-electron mass  $m_e$ , are presented in Fig. 7(a) for different  $N$ , plotted as a function of energy. The solid curve is the effective mass calculated from the projected bulk band structure; this is equivalent to assuming that the phase shift  $\varphi_i + \varphi_s$  is independent of the parallel component of the momentum of the electron. The bulk band results are seen to correspond closely to the experimental results. The effective masses in Pb/HOPG are thus quite normal. The results imply that the phase shift is indeed nearly independent of the parallel component of the electron momentum. This is reasonable as the band gap of graphite is very large near the zone center, and coupling between the Pb  $p$  band with the substrate electronic states is expected to be weak. Since the Pb-graphite interface is incommensurate, accurate calculations of the phase-shift function would be difficult and are currently unavailable.

By contrast, anomalously large effective masses, and even negative effective masses, have been reported in a number of systems including Cu/Co(001),<sup>32</sup> Ag/V(100),<sup>33</sup> Ag/Si(111), Ag/Si(100),<sup>11</sup> Cu/Co/Cu(001),<sup>34</sup> and Pb/Si(111).<sup>14,15</sup> The common occurrence has suggested possibly a generic explanation. In one proposal,<sup>14</sup> lateral electron localization was put forth as the cause for the enhanced effective masses in Pb/Si. This localization idea was also proposed earlier in a scanning tunneling microscopy study of the same system.<sup>35</sup> Conceptually, localization could occur in thin films for two possible reasons. One is that the confined geometry could force overlap of the wave functions, resulting in enhanced correlation effects and a modified dispersion relation. The other is that interfacial scattering in incommensurate film systems could potentially lead to Anderson-type localization.

Our results for Pb/HOPG rule out the first of the two interpretations because the same confined geometry in Pb/

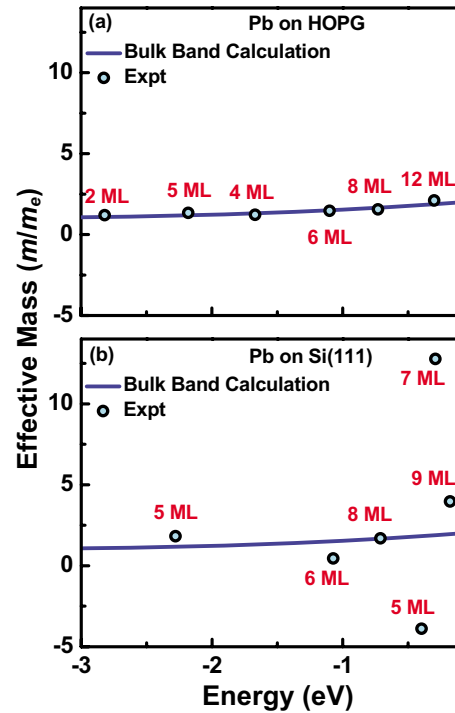


FIG. 7. (Color online) Measured effective masses at the zone center as a function of energy for (a) Pb films on HOPG and (b) Pb films on Si(111). The results are normalized to the free-electron mass  $m_e$ . The solid curve in each panel is derived from a calculation based on the projected bulk band structure of Pb; this is what one should observe when interfacial effects are negligible.

HOPG does not yield enhanced effective masses. The lattice mismatch between Pb and HOPG is large, about 30%. However, the interaction between Pb and HOPG is relatively weak; so interface scattering could be weak. For this reason, the Pb/HOPG results do not necessarily address the question of Anderson localization.

Another interpretation of the anomalous effective masses in Pb/Si is a hybridization interaction between the film and substrate electronic structures.<sup>15</sup> It has been shown that such hybridization interaction can substantially modify the QWS subband dispersion relations, resulting in anomalous effective masses near the substrate band edge. The data for Pb/Si from a previous study are presented in Fig. 7(b) for comparison.<sup>15</sup> Indeed, the anomalous behavior is quite pronounced, but only near the Si band edge. Furthermore, it has been demonstrated that a QWS subband crossing the substrate band edge can even split into two pieces under certain conditions, thus making an analysis based on Eq. (1) dubious.<sup>12</sup> One should generally speak of a spectral function associated with the combined film-substrate system instead of treating the film as an independent quantum well system, with the substrate effects simply included as a phase shift. The Pb/HOPG results are fully consistent with this interpretation. Because of the weak electronic interaction at the interface and the large gap in HOPG near  $\bar{\Gamma}$ , the effective masses are little affected by the substrate electronic structure.

#### IV. CONCLUDING REMARKS

This study is to explore and document the electronic structure and growth behavior of Pb films on HOPG, and to examine the relevant physics in terms of quantum well effects. The growth mode is found to be a good example of electronic growth, for which electronic energy minimization leads to preferred film thicknesses. Despite the three-dimensional growth with several film thicknesses present simultaneously, it is possible to make a unique assignment for each of the QWS peaks in terms of a quantum number and the exact film thickness in atomic layers. Overall, the electronic structure of Pb/HOPG is well described by a weakly interacting interface, with the results closely resembling those for freestanding films based on a first-principles calculation. The energies of the QWSs are fairly close to those in Pb/SiC, but several peaks observed in Pb/HOPG are completely missing in Pb/SiC. Comparing Pb/HOPG with Pb/Si, there are significant differences in the quantum well electronic structure. The total energies also differ, leading to the different preferred film thicknesses in these two systems. The effective masses at the zone center are also very different,

with the results for Pb/HOPG being normal (bulklike), while those for Pb/Si being anomalous. As graphene sheets and stacks are gaining interest for possible electronic applications, the present work provides useful basic information about the formation of interfaces and films involving a simple prototypical metal.

#### ACKNOWLEDGMENTS

This work was supported by the U.S. Department of Energy (Grant No. DE-FG02-07ER46383). We acknowledge the Petroleum Research Fund, administered by the American Chemical Society, and the U.S. National Science Foundation (Grant No. DMR-05-03323) for partial support of the personnel and the beamline facilities at the Synchrotron Radiation Center. The Synchrotron Radiation Center is supported by the U.S. National Science Foundation (Grant No. DMR-05-37588). The tight-binding code used for the bulk band-structure calculation in this study was provided by M. J. Mehl of the Naval Research Laboratory under the U.S. Department of Defense CHSSI program.

- 
- <sup>1</sup>T. Miller, A. Samsavar, G. E. Franklin, and T.-C. Chiang, *Phys. Rev. Lett.* **61**, 1404 (1988).
- <sup>2</sup>T.-C. Chiang, *Surf. Sci. Rep.* **39**, 181 (2000).
- <sup>3</sup>F. J. Himpsel, J. E. Ortega, G. J. Mankey, and R. F. Willis, *Adv. Phys.* **47**, 511 (1998).
- <sup>4</sup>M. Milun, P. Pervan, and D. P. Woodruff, *Rep. Prog. Phys.* **65**, 99 (2002).
- <sup>5</sup>T.-C. Chiang, *Science* **306**, 1900 (2004).
- <sup>6</sup>T. Miller, A. Samsavar, and T.-C. Chiang, *Phys. Rev. B* **50**, 17686 (1994).
- <sup>7</sup>S.-J. Tang, Y.-R. Lee, S.-L. Chang, T. Miller, and T.-C. Chiang, *Phys. Rev. Lett.* **96**, 216803 (2006).
- <sup>8</sup>P. Moras, L. Ferrari, C. Spezzani, S. Gardonio, M. Ležaić, P. Mavropoulos, S. Blügel, and C. Carbone, *Phys. Rev. Lett.* **97**, 206802 (2006).
- <sup>9</sup>Y. Liu, N. J. Speer, S.-J. Tang, T. Miller, and T.-C. Chiang, *Phys. Rev. B* **78**, 035443 (2008).
- <sup>10</sup>L. Aballe, C. Rogero, P. Kratzer, S. Gokhale, and K. Horn, *Phys. Rev. Lett.* **87**, 156801 (2001).
- <sup>11</sup>I. Matsuda, T. Ohta, and H. W. Yeom, *Phys. Rev. B* **65**, 085327 (2002).
- <sup>12</sup>S.-J. Tang, L. Basile, T. Miller, and T.-C. Chiang, *Phys. Rev. Lett.* **93**, 216804 (2004).
- <sup>13</sup>N. J. Speer, S.-J. Tang, T. Miller, and T.-C. Chiang, *Science* **314**, 804 (2006).
- <sup>14</sup>J. H. Dil, J. W. Kim, T. Kampen, K. Horn, and A. R. H. F. Ettema, *Phys. Rev. B* **73**, 161308(R) (2006).
- <sup>15</sup>M. H. Upton, T. Miller, and T.-C. Chiang, *Phys. Rev. B* **71**, 033403 (2005).
- <sup>16</sup>M. H. Upton, C. M. Wei, M. Y. Chou, T. Miller, and T.-C. Chiang, *Phys. Rev. Lett.* **93**, 026802 (2004).
- <sup>17</sup>A. Mans, J. H. Dil, A. R. H. F. Ettema, and H. H. Weitering, *Phys. Rev. B* **66**, 195410 (2002).
- <sup>18</sup>See, for example, A. K. Geim and K. S. Novoselov, *Nature Mater.* **6**, 183 (2007).
- <sup>19</sup>J. H. Dil, T. U. Kampen, B. Hülsen, T. Seyller, and K. Horn, *Phys. Rev. B* **75**, 161401(R) (2007).
- <sup>20</sup>F. Patthey and W.-D. Schneider, *Phys. Rev. B* **50**, 17560 (1994).
- <sup>21</sup>G. Neuhold and K. Horn, *Phys. Rev. Lett.* **78**, 1327 (1997).
- <sup>22</sup>M. Breitholtz, T. Kihlgren, S.-Å. Lindgren, H. Olin, E. Wahlström, and L. Walldén, *Phys. Rev. B* **64**, 073301 (2001).
- <sup>23</sup>M. Breitholtz, T. Kihlgren, S.-Å. Lindgren, and L. Walldén, *Phys. Rev. B* **67**, 235416 (2003).
- <sup>24</sup>A. W. Moore, in *Chemistry and Physics of Carbon*, edited by J. Philip, L. Walker, and P. A. Thrower (Dekker, New York, 1973).
- <sup>25</sup>S. Hüfner, *Photoelectron Spectroscopy*, 2nd ed. (Springer-Verlag, New York, 1996).
- <sup>26</sup>M. E. Dávila, M. A. Valbuena, V. Pantín, J. Avila, P. Esquinazi, and M. C. Asensio, *Appl. Surf. Sci.* **254**, 55 (2007).
- <sup>27</sup>C. M. Wei and M. Y. Chou, *Phys. Rev. B* **66**, 233408 (2002).
- <sup>28</sup>M. C. Tringides and M. Hupalo, *Phys. Rev. Lett.* **94**, 079701 (2005); M. H. Upton, T. Miller, and T.-C. Chiang, *ibid.* **94**, 079702 (2005).
- <sup>29</sup>H. Hong, C. M. Wei, M. Y. Chou, Z. Wu, L. Basile, H. Chen, M. Holt, and T.-C. Chiang, *Phys. Rev. Lett.* **90**, 076104 (2003).
- <sup>30</sup>H. Hong, L. Basile, P. Czoschke, A. Gray, and T.-C. Chiang, *Appl. Phys. Lett.* **90**, 051911 (2007).
- <sup>31</sup>K. Budde, E. Abram, V. Yeh, and M. C. Tringides, *Phys. Rev. B* **61**, R10602 (2000).
- <sup>32</sup>P. D. Johnson, K. Garrison, Q. Dong, N. V. Smith, Dongqi Li, J. Mattson, J. Pearson, and S. D. Bader, *Phys. Rev. B* **50**, 8954 (1994).
- <sup>33</sup>T. Valla, P. Pervan, M. Milun, A. B. Hayden, and D. P. Woodruff, *Phys. Rev. B* **54**, 11786 (1996).
- <sup>34</sup>Y. Z. Wu, C. Y. Won, E. Rotenberg, H. W. Zhao, F. Toyoma, N. V. Smith, and Z. Q. Qiu, *Phys. Rev. B* **66**, 245418 (2002).
- <sup>35</sup>I. B. Altfeder, X. Liang, T. Yamada, D. M. Chen, and V. Narayanamurti, *Phys. Rev. Lett.* **92**, 226404 (2004).